Available online at www.sciencedirect.com
ScienceDirect
Journal of Sound and Vibration 313 (2008) 149–170
JOURNAL OF SOUND AND VIBRATION
www.elsevier.com/locate/jsvi

Stochastic modelling of traffic-induced building vibration ☆

Y.L. Xu*, X.J. Hong

Department of Civil and Structural Engineering, The Hong Kong Polytechnic University, Kowloon, Hong Kong, China

Received 29 July 2006; received in revised form 12 August 2007; accepted 11 November 2007
Available online 27 December 2007

Abstract

Because of rapid urbanization, more and more buildings are constructed closer to roadsides than they used to be. This gives rise to some environmental problems, for traffic-induced ground vibration deteriorates the human comfort in neighbouring buildings and affects the normal operation of nearby high-tech facilities. This paper presents a framework for quantifying traffic-induced building vibration in a stochastic way. Vehicle distribution along a roadway is first simulated based on vehicle spacing distribution and vehicle-type distribution. In consideration of buildings in proximity to the roadway, not only Rayleigh waves but also body waves induced by moving vehicle forces are included in the determination of the frequency-response function of a half-space. The combination of the moving force spectra with the frequency-response function of the half-space then leads to evolutionary ground spectra. The framework further provides a method for deriving the evolutionary spectra of a building to the evolutionary ground spectra. The proposed framework is finally applied to a typical three-dimensional high-tech facility, in which the effects of both a single heavy truck and a two-way traffic flow on building vibration are investigated. The results show that traffic-induced ground vibration impedes the normal operation of the high-tech facility.

1. Introduction

Owing to rapid urbanization and high-density development of infrastructures in urban districts, more and more buildings are constructed closer to roadway or railway than they used to be. This brings out some environmental problems because traffic-induced ground motions may cause neighbouring buildings vibrate, deteriorate human comfort, and affect the normal operations of high-tech facilities. Many investigations have therefore been conducted to ascertain the mechanism of traffic-induced ground motion and its effects on human comfort and sensitive equipment in buildings [1–11].

The mechanism of generation and transmission of traffic-induced ground vibration is complex in nature. The theoretical and numerical methods such as wave propagation theory, finite element method, and boundary element method were employed to simulate ground vibrations due to highway or railway traffic. Auersch [1] employed a method of numerical integration in the wavenumber domain to calculate the wave

☆The work described in this paper was financially supported by the Research Grants Council of Hong Kong (Project No. PolyU5054/02E).

*Corresponding author. Tel.: +852 27666050; fax: +852 23346389.
E-mail addresses: ceylxu@polyu.edu.hk (Y.L. Xu), cehongxj@polyu.edu.hk (X.J. Hong).

0022-460X/$ - see front matter © 2007 Elsevier Ltd. All rights reserved.
doi:10.1016/j.jsv.2007.11.031

field of horizontally layered soil. Hanazato and Ugai [2] used a finite element method to simulate ground vibrations transmitted from a road on a layered site subjected to harmonic forces. Based on the dynamic substructure method, the boundary element method was utilized to deal with the numerical modelling of free field vibrations induced during the passage of a vehicle [3–5]. The random vibration methods were also used to calculate the power spectra of road vehicle-induced ground vibration based on the assumption that vehicles were sufficiently closely spaced so that ground vibration could be considered to be a stationary random process [6,7]. By adopting the same assumption but using a single-axle two-degrees-of-freedom vehicle model, Hao and Ang [8] derived a closed-form solution for the power spectrum of traffic-induced ground vibration. Hao et al. [9] then analysed dynamic responses of five hypothetical two-dimensional reinforced concrete structures subjected to field measured ground motions caused by a normal road traffic flow. Watts and Krylov [10] even derived empirical relations for advisable minimum distances of buildings to roads on different types of soil by studying ground-borne vibrations due to the passage of different types of vehicles at various speeds on several types of road unevenness. Nevertheless, only Rayleigh waves were considered in the preceding studies when deriving the frequency-response functions for a half-space with the assumption that the motion felt on the surface of the half-space at a large distance from the applied impulse is due mostly to the propagation of Rayleigh waves. These studies are well suited to ascertaining road traffic-induced ground motions as well as building vibrations in the frequency domain when the ground motions and building vibrations concerned are at a distance significantly greater than the mean vehicle spacing and the assumptions of the stationary ground motion and stationary building responses can be accepted [3,7,8].

This study concerns road traffic-induced vibrations of buildings and high-tech facilities in proximity to roadways. The effects of body waves (shear and compressive waves) on ground vibrations should not be ignored. This study not only concerns a single heavy truck but also a traffic flow on a multi-lane roadway. The ground motions due to road traffic are non-stationary and the evolutionary ground motion spectra should be determined as the level of vibration rises and falls with passages of vehicles. Furthermore, most of the previous studies focus on traffic-induced ground motion, and traffic-induced building vibrations are less investigated. This paper aims at presenting a framework for quantifying traffic-induced building vibration in a stochastic way. Vehicle distribution along a roadway is first simulated based on vehicle spacing distribution and vehicle-type distribution. In consideration of buildings in proximity to the roadway, not only Rayleigh waves but also body waves induced by moving vehicle forces are included in the determination of the frequency-response function of an elastic half-space. The combination of the moving force spectra with the frequency-response function of the half-space then leads to evolutionary ground response spectra. The framework further provides a method for deriving the evolutionary spectra of building responses from the evolutionary ground spectra. The proposed framework is finally applied to a typical three-dimensional high-tech facility, in which the effects of both a single heavy truck and a two-way traffic flow on building vibrations are investigated. To assess the performance of the high-tech facility against traffic-induced ground vibrations, the Bolt, Beranek and Newman (BBN) criteria [12], which are widely adopted for the assessment of stationary environmental vibration problems, are extended in this study for the evolutionary spectra of building responses.

2. Traffic flow simulation

This study concerns traffic-induced vibration of a building in proximity to a busy multi-lane road. The spacing between two adjacent vehicles in one lane may not be large enough to allow considering the worst case of a single vehicle passage only with confidence. It is also possible in practice that vehicle queues on two or more lanes pass by the investigation point in either same or opposite directions at almost the same time. Therefore, the traffic flow or vehicle distribution along a multi-lane road is simulated in this section so that the building responses due to different types of excitation such as a single heavy truck and a two-way traffic flow could be investigated.

By assuming the random Gaussian vehicle spacing about a mean value and the random Gaussian vehicle mass distribution about a mean value with a standard deviation, Hunt [6] presented a single-axle vehicle distribution along a roadway. The mass ratio, characteristic frequencies and damping ratio of all types of vehicles on a given road were assumed to be the same. To refine this model for considering buildings in

proximity to roadside, the vehicle spacing distribution used in this study is based on a Poisson arrival process [13] while vehicle-type distribution is given by a statistical analysis with reference to Refs. [8,14].

2.1. Vehicle spacing distribution

By assuming that one lane traffic flow is expedite without the influence of traffic signals and other factors which may result in traffic congest and the traffic flow density (the number of vehicles passing by within unit time) can be deemed invariant within the simulation period of ground motion, the number of vehicles arriving at a fixed point within a duration [0, t] can then be described by the Poisson distribution function:

$$P(n = N) = \frac{(\overline{\lambda}t)^N}{N!}\exp(-\overline{\lambda}t), \tag{1}$$

where $\overline{\lambda}$ is the flow density and N the number of vehicles arriving at the concerned point during the time interval [0, t]. By assuming that all vehicles in one lane run at a constant velocity V, Eq. (1) yields the vehicle spacing distribution function as

$$P(\Delta S_1 \leqslant s) = 1 - \exp\left(-\overline{\lambda}\frac{s}{V}\right) \tag{2}$$

in which V is the traffic flow velocity and ΔS_1 is the spacing between two adjacent vehicles. For safety reason, the vehicle spacing ΔS_1 should not be less than a threshold value Δ_d. Accordingly, the function described by Eq. (2) should be modified as

$$P(\Delta S_1 \leqslant s) = \begin{cases} 1 - \exp\left(-\dfrac{\overline{\lambda}}{V}(s - \Delta_d)\right) & (s \geqslant \Delta_d), \\ 0 & (s < \Delta_d) \end{cases} \tag{3}$$

in which $\Delta_d = V\Delta t_r$ and Δt_r is the minimum reaction time allowed for a driver. In the following analysis, Δ_d is taken as a constant value for a given constant traffic flow velocity.

2.2. Vehicle-type distribution

In this study, the vehicle-type distribution is determined based on the statistical analysis of traffic records from a particular roadway within a period [0, t]. All vehicles running on the road are approximately classified into five types: car, minibus, bus, truck, and heavy truck. The characteristics of vehicles in each type are assumed to be the same and listed in Table 1 with reference to the information provided in Refs. [8,14]. The characteristics of vehicles listed in Table 1 include weight, mass ratio, body-bounce frequency, body-bounce damping ratio, wheel-hop frequency, and wheel-hop damping ratio. Based on traffic surveying records, the occurrence probability and its corresponding probability distribution function of vehicle type within the

Table 1
Vehicle types and properties

	Weight (t)	Mass ratio	F_b (Hz)	ξ_b	F_h (Hz)	ξ_h
Car	2	0.15	1.5	0.05	10	0.3
Minibus	10	0.15	1.7	0.07	10	0.3
Bus	20	0.15	1.7	0.07	11	0.3
Truck	25	0.15	1.5	0.04	8	0.3
Heavy truck	32	0.15	2.0	0.04	17	0.3

concerned time period can be expressed as

$$\begin{cases} f(T_e =' \text{car}') = p_1, \\ f(T_e =' \text{minibus}') = p_2, \\ f(T_e =' \text{bus}') = p_3, \\ f(T_e =' \text{truck}') = p_4, \\ f(T_e =' \text{heavy truck}') = p_5, \end{cases} \qquad P(T_e) = \begin{cases} p_1, & T_e \in c, \\ p_1 + p_2, & T_e \in c \cup m, \\ p_1 + p_2 + p_3, & T_e \in c \cup m \cup b, \\ p_1 + p_2 + p_3 + p_4, & T_e \in c \cup m \cup b \cup t, \\ 1, & T_e \in c \cup m \cup b \cup t \cup h, \end{cases} \tag{4}$$

where T_e stands for vehicle type, and c, m, b, t, h represents car, minibus, bus, truck, and heavy truck, respectively.

2.3. Vehicle distribution along a roadway

This study assumes that vehicle spacing and vehicle type are independent of each other. The vehicle distribution along a roadway can be numerically generated by the method described as below. Draw a line perpendicular to the roadway through the investigated point (building location) to have point o and then take point o as the origin point, as shown in Fig. 1. The coordinate x_o of the first vehicle is assumed to be evenly distributed within the section $[-(1/2)E(S)(1/2)E(S)]$ and determined by

$$x_o = \left(U - \tfrac{1}{2}\right)E(s) \tag{5}$$

in which $E(s)$ is the mean value of the vehicle spacing equal to $\Delta_d + V/\bar{\lambda}$; and U is the random variable evenly distributed within the range [0 1]. The vehicle spacing between two adjacent vehicles can be generated using the inverse transform of Eq. (3) [15]:

$$\Delta S_1 = V\frac{\log(1-U)}{-\bar{\lambda}} + \Delta_d. \tag{6}$$

With reference to the coordinate x_o and the spacing of the adjacent vehicles, the coordinates of other vehicles can be deduced by

$$\begin{cases} x_1 = x_o + \Delta S_1, & x_{-1} = x_o - \Delta S_{-1}, \\ \vdots & \\ x_m = x_{m-1} + \Delta S_m, & x_{-n} = x_{-n+1} - \Delta S_{-n}. \end{cases} \tag{7}$$

The vehicle queue length simulated in the roadway should be long enough so that the movement of the vehicles at the two ends of the traffic flow will not significantly affect the traffic-induced ground motion at the investigation point. Once the vehicle queue in the roadway is determined, the type of vehicle can be assigned to

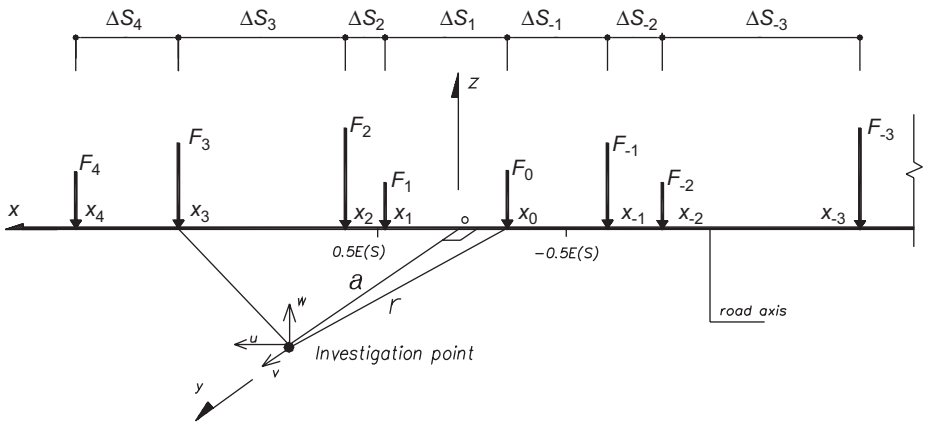

Fig. 1. Coordinate system for describing vehicle-induced ground motion.

each vehicle position. This is done by generating a random variable U evenly distributed within the range [0 1] and then determining the vehicle type according to U and Eq. (4). For instance, if U satisfies the condition $P_1+P_2<U\leqslant P_1+P_2+P_3$, the vehicle type is "bus". After the vehicle distribution along the roadway is completely generated, all the vehicles in the queue are assumed to move together at a constant velocity V. This method can be applied to each lane in a road to simulate two or more vehicle queues in either the same direction or the opposite direction.

3. Vehicle-induced ground vibration

3.1. Vehicle-induced force spectra

Various vehicle models have been developed to analyse vehicle response and assess vehicle performance. Since the primary concern in the present study is to calculate vehicle force-induced ground motion other than the assessment of vehicle performance, the simplest single-axle two-degrees-of-freedom vehicle model, as shown in Fig. 2 and used in the literatures [6,8], is employed to facilitate the consideration of traffic flow-induced ground motion. The equation of motion of a vehicle in the traffic flow is given as

$$\begin{bmatrix} m_1 & 0 \\ 0 & m_2 \end{bmatrix}\begin{bmatrix} \ddot{x}_1 \\ \ddot{x}_2 \end{bmatrix}+\begin{bmatrix} c_1 & -c_1 \\ -c_1 & c_1+c_2 \end{bmatrix}\begin{bmatrix} \dot{x}_1 \\ \dot{x}_2 \end{bmatrix}+\begin{bmatrix} k_1 & -k_1 \\ -k_1 & k_1+k_2 \end{bmatrix}\begin{bmatrix} x_1 \\ x_2 \end{bmatrix}=\begin{bmatrix} 0 \\ c_2\dot{y}+k_2y \end{bmatrix}, \tag{8}$$

where x_1 and x_2 are the displacement responses of the vehicle body and the axle, respectively; y is the road surface roughness; m_1 and m_2 are the masses of vehicle body and wheel (plus tyre), respectively; k_1 and k_2 are the vehicle suspension and tire spring constants, respectively; and c_1 and c_2 are the vehicle suspension and tire damping constants, respectively. The power spectral density (PSD) function of the vehicle force is then given by

$$S_{ff}(\omega)=\frac{1}{V}S_d\left(\frac{\omega}{2\pi V}\right)|H_{fd}(\mathrm{i}\omega)|^2, \tag{9}$$

where H_{fd} (iω) is the frequency-response function of vehicle force to road surface roughness, which can be denoted by H_{fd} (iω) $=m_1\omega^2[X_1(\mathrm{i}\omega)+\mu X_2(\mathrm{i}\omega)]$; i is the imagination unit equal to $\sqrt{-1}$; μ is the mass ratio m_2/m_2; X_1 and X_2 are the frequency transformation of x_1 and x_2, respectively; and S_d is the displacement PSD function of the road surface roughness [16]. This study assumes that the correlation between moving vehicle forces due to the road surface roughness is insignificant. Thus, the traffic flow-induced ground motion is the summation of the ground motion induced by each vehicle in the traffic flow.

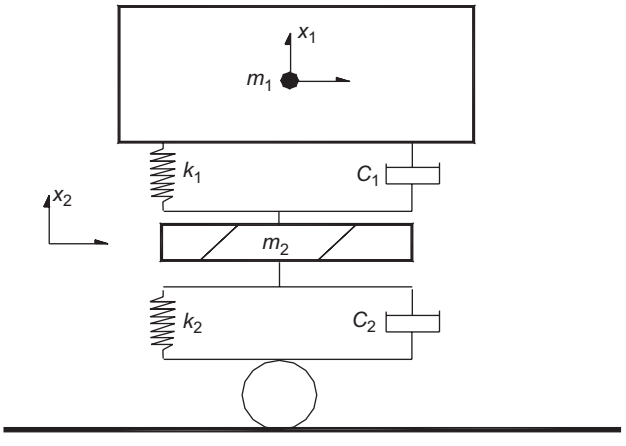

Fig. 2. Single-axle vehicle model.

3.2. Half-space frequency-response function

Consider one single harmonic point force $F_o(t) = F_o \exp(\mathrm{i}\omega t)$ acting vertically on the surface of a half-space at a coordinate x_o from the origin o producing a disturbance within the half-space (see Fig. 1). The distance between the applied force and the investigation point (building location) is $r = \sqrt{x_o^2 + a^2}$, in which a is the perpendicular distance of the investigation point to the roadway. The radial and vertical components of the surface displacements at the investigation point in response to $F_o(t)$ are denoted, respectively, by $q(r,t) = q(r)\exp(\mathrm{i}\omega t)$ and $w(r,t) = w(r)\exp(\mathrm{i}\omega t)$. The corresponding frequency-response functions can be written as

$$\begin{cases} H_{qf}(r,\omega) = q(r)/F, \\ H_{wf}(r,\omega) = w(r)/F. \end{cases} \tag{10}$$

Disturbances within a homogenous, isotropic half-space propagate through the body of the half-space as body waves and along the surface as Rayleigh waves. The general formulae of the surface displacement responses, including the effects of both body waves and Rayleigh waves, to a vertical harmonic point force can be found in Ref. [17], but the general solution could not be found because of the singularity in the general formulae. It is well known that body waves generally decay inversely as the square of the distance from the point of excitation while Rayleigh waves decay inversely as the square root of the distance. The surface response will therefore be progressively dominated by Rayleigh waves as the distance from the excitation point increases. When the investigation point is far away from the excitation point as concerned in most of the previous studies, the surface displacement responses considering Rayleigh waves only can be accepted and the solution of frequency-response functions for this case can be found in Ref. [8]. When the investigation point is close to the excitation point or in the near field as concerned in this study, only considering Rayleigh wave effects may lead to the underestimation of the response. Holzlohner [18] overcame the difficulties due to the singularity in the general formulae presented in Ref. [17] by choosing an appropriate method of superposition and found out the solution for the surface displacement responses including the effects of both Rayleigh waves and body waves:

$$\begin{cases} q(r,t) = \dfrac{F_o \exp(\mathrm{i}\omega t)}{Gr} p_q(r, \mathrm{i}\omega), \\ w(r,t) = \dfrac{F_o \exp(\mathrm{i}\omega t)}{Gr} p_w(r, \mathrm{i}\omega) \end{cases} \tag{11a}$$

in which P_q and P_w are denoted, respectively, by

$$p_q = \frac{\mathrm{i}\bar{r}k}{2} B H_1^{(2)}(\bar{r}k) + \frac{\mathrm{i}\bar{r}}{\pi}\left(\int_h^1 \frac{x^2(2x^2-1)\sqrt{1-x^2}\sqrt{x^2-h^2}}{(2x^2-1)^4 + 16(x^2-h^2)(1-x^2)x^4} H_1^{(2)}(\bar{r}x)\,\mathrm{d}x \right), \tag{11b}$$

$$\begin{aligned} p_w = {} & 8\left(\int_h^1 \frac{\sqrt{1-x^2}(x^2-h^2)x^2}{(2x^2-1)^4 + 16(x^2-h^2)(1-x^2)x^4} \phi(\bar{r}x)\,\mathrm{d}x \right) \\ & + 2\left(\int_0^h \frac{\sqrt{h^2-x^2}}{(2x^2-1)^2 + 4x^2\sqrt{(h^2-x^2)(1-x^2)}} \phi(\bar{r}x)\,\mathrm{d}x \right) \\ & + \frac{2\pi(2k^2-1)^2\sqrt{k^2-h^2}}{8k(1-(6-4h^2)k^2+6(1-h^2)k^4)} \phi(\bar{r}k), \end{aligned} \tag{11c}$$

where G is the shear modulus of the soil medium, k the real root of equation $(2x^2-1)^2 - 4x^2\sqrt{x^2-h^2}\sqrt{x^2-1} = 0$, h the ratio of the shear wave velocity to the compressive wave velocity, defined as $\sqrt{(1-2v)/(2-2v)}$, v the Poisson ratio of soil medium; $\bar{r}$ is the dimensionless frequency defined as $\omega r/C_s$, C_s the shear wave velocity of the half-space, $H_1^{(2)}$ the Hankel function of second kind and first order, and the

function $\phi(\bar{r}x)$ and the value B can be found in Ref. [18]. Holzlohner [18] pointed out that the function p_w can be used up to $\bar{r} = 40$, beyond which the solution for far field can be used.

With the radial displacement resolved into its Cartesian components, the frequency-response functions of the horizontal displacement components u and v can be obtained:

$$\begin{cases} H_{uf}(r,\omega) = \dfrac{-x_0}{r} H_{qf}(r,\omega), \\ H_{vf}(r,\omega) = \dfrac{a}{r} H_{qf}(r,\omega). \end{cases} \tag{12}$$

The preceding frequency-response functions are derived without considering soil damping. By considering hysteretic damping, which is commonly used to model soil energy loss in previous studies, the frequency-response function of a damped system can be obtained from that of an elastic system by writing the elastic moduli as complex quantities [8]. For instance, Eq. (11) can be used to approximately include the effect of soil damping by replacing G by $\bar{G} = G(1 + 2\mathrm{i}\xi)$ and C_s by $\bar{C}_s = C_s\sqrt{1 + 2\mathrm{i}\xi}$ where ξ is the damping ratio of soil.

3.3. Evolutionary spectra of ground motion

In this study, buildings or high-tech facilities at the investigation point are in proximity to the roadway. The ground vibration caused by the road traffic at the investigation point cannot be considered as a stationary random process, for the distance of each vehicle force to the investigation point varies with time as the N vehicle forces move forward. Therefore, when N vehicle forces $F_1, F_2, \ldots, F_N$ act on the road, the power spectra of the ground surface displacement at the investigation point due to N vehicle forces vary with time, leading to the evolutionary power spectra:

$$S_{R_iR_j}(\omega,t) = \sum_{k=1}^{N} H^*_{R_if_k}(x_k,t) H_{R_jf_k}(x_k,t) S_{f_kf_k}(\omega) \quad (R_i, R_j = u, v, w), \tag{13}$$

where $x_k(t)$ is the coordinate of vehicle force $F_k(t)$, $H_{R_jf_k}(x_k,t)$ is the frequency-response function of R_j to the kth vehicle force (see Eqs. (10) and (12)), the superscript * in Eq. (13) signifies the complex conjugate, $S_{f_kf_k}(\omega)$ is the power spectrum of the kth vehicle force $F_k(t)$ (see Eq. (9)). The initial coordinates of the N vehicle forces at the time $t = 0$ can be generated in terms of Eqs. (6) and (7) together with the vehicle distribution along the roadway. As a result and considering a multi-lane road, the coordinate of the kth vehicle in the ith lane at time t can be deduced by $x_{k,i}(t) = x_{k,i}(0) + V_i t$, where $x_{k,i}(t)$ is the coordinate of the kth vehicle in the ith lane at time t and V_i is the traffic flow velocity on the ith lane.

4. Traffic-induced building vibration

4.1. Evolutionary spectra and building responses

Since traffic-induced ground motions are time dependent and described by evolutionary spectra, traffic-induced building responses are also estimated in the frequency domain in terms of evolutionary spectra and variance in this study. Considering that the performance of a high-tech building against traffic-induced vibration is often assessed in terms of the absolute velocity responses of building floors [12], the equation of motion of the building with multiple supports subjected to ground motion is first established in the absolute coordinate in partitioned form and the second of the two partitioned equations is then selected to form the following governing equation of motion for the superstructure of the building [19]:

$$\mathbf{M}\ddot{\mathbf{x}} + \mathbf{C}\dot{\mathbf{x}} + \mathbf{K}\mathbf{x} = -\mathbf{M}_s^{\mathrm{t}}\ddot{\mathbf{x}}_s - \mathbf{C}_s^{\mathrm{t}}\dot{\mathbf{x}}_{\mathbf{s}} - \mathbf{K}_s^{\mathrm{t}}\mathbf{x}_{\mathbf{s}}, \tag{14}$$

where $\mathbf{x}_s$ is the absolute displacement vector of the building supports, $\mathbf{x}$ is the absolute displacement of the building, $\mathbf{M}_s$, $\mathbf{C}_s$, $\mathbf{K}_s$ are the mass, damping, and stiffness matrix, respectively, of the building supports, $\mathbf{M}$, $\mathbf{C}$, $\mathbf{K}$ are the mass, damping, and stiffness matrix, respectively, of the building, t denotes the transpose of a matrix. All the mass, damping, and stiffness matrices can be determined from the properties of the building using the conventional finite element method. Assume that the building foundation is rigid and the building

supports are subjected to the same ground motion in the x-, y- and z-direction, respectively. The displacement of building supports can be expressed as $\mathbf{x}_s = T\,[u,v,w]^{\mathrm{t}}$, where u, v, w are the ground displacements in the x-, y- and z-direction, respectively, and $\boldsymbol{T}$ is the transformation matrix converting the ground motions to the support motions:

$$\mathbf{T} = \begin{bmatrix} 1 & 0 & 0 & 0 & 0 & 0 & \dots & 1 & 0 & 0 & 0 & 0 & 0 & \dots \\ 0 & 1 & 0 & 0 & 0 & 0 & \dots & 0 & 1 & 0 & 0 & 0 & 0 & \dots \\ 0 & 0 & 1 & 0 & 0 & 0 & \dots & 0 & 0 & 1 & 0 & 0 & 0 & \dots \end{bmatrix}^{\mathrm{t}}. \tag{15}$$

To facilitate the performance assessment of a high-tech facility subject to traffic-induced vibration, the motion of the superstructure is reformulated in state space form as

$$\begin{cases} \dot{\mathbf{y}} = \mathbf{A}\mathbf{y} + \mathbf{B}\mathbf{E}, \\ \mathbf{v} = \mathbf{S}\mathbf{y} \end{cases} \tag{16}$$

in which $\boldsymbol{y}$ is the state vector denoted by $\mathbf{y} = [\mathbf{x},\ \dot{\mathbf{x}}]^{\mathrm{t}}$, $\mathbf{v}$ the selected building velocity response vector, and $\mathbf{S}$ the corresponding selection matrix. The impulse response matrix immediately follows $\mathbf{H}(t) = \mathbf{S}\exp(At)\mathbf{B}$, and the absolute velocity response vectors are then given by

$$\mathbf{v}(t_i) = \int_0^{t_i} \mathbf{H}(t_i - s_i)\mathbf{E}(s_i)\,\mathrm{d}s_i \quad (i = 1, 2). \tag{17}$$

Let us find the absolute velocity response v_k of the building at the kth dof. The selection matrix $\mathbf{S}$ is then denoted as $\mathbf{S} = [\underset{1}{0}, \underset{2}{0}, \dots \underset{k}{0}, \dots \underset{n}{0}, \underset{n+1}{0}, 0, \dots \underset{n+k}{1}, \dots \underset{2n}{0}]$ in which n is the number of degrees of freedom of the building. The autocorrelation function of the velocity response v_k is then given as

$$\begin{aligned} E(v_k(t_1)v_k(t_2)) &= \int_0^{t_2}\int_0^{t_1} \mathbf{H}(t_1 - s_1)E(\mathbf{E}(s_1)\mathbf{E}^{\mathrm{t}}(s_2))\mathbf{H}^{\mathrm{t}}(t_2 - s_2)\,\mathrm{d}s_1\,\mathrm{d}s_2 \\ &= \int_{-\infty}^{\infty} \sum_l \sum_j \int_0^{t_1}\int_0^{t_2} h_{kl}(t_1 - s_1)\exp(-\mathrm{i}\omega s_1)h_{kj}(t_2 - s_2) \\ &\quad \times \exp(\mathrm{i}\omega s_2)S_{lj}(\omega, s_1, s_2)\,\mathrm{d}s_1\,\mathrm{d}s_2\,\mathrm{d}\omega \end{aligned} \tag{18}$$

in which h_{kl} is the impulse response function at the kth dof of the building due to a unit ground impulse in the lth direction, and $S_{lj}(\omega,\ s_1,\ s_2)$ $(l,j = u, v, w, \dot{u}, \dot{v}, \dot{w}, \ddot{u}, \ddot{v}, \ddot{w})$ is the cross-spectrum of the lth and jth ground motion components. For a non-stationary process such as traffic-induced ground displacement discussed in this study, the Riemman–Stieltje integral [20] can be extended to

$$g(t) = \int_{-\infty}^{\infty} A_g(\omega, t)\exp(\mathrm{i}\omega t)\,\mathrm{d}g(\omega) \quad (g(t) = u, v, w) \tag{19}$$

in which $A_g(\omega,t)$ is the definite modulation function depending on frequency and time. Accordingly, the traffic-induced ground velocity and acceleration can be expressed as

$$\begin{cases} \dot{g}(t) = \int_{-\infty}^{\infty} B_g(\omega, t)\exp(\mathrm{i}\omega t)\,\mathrm{d}g(\omega) = \int_{-\infty}^{\infty}(\dot{A}_g(\omega, t) + \mathrm{i}\omega A_g(\omega, t))\exp(\mathrm{i}\omega t)\,\mathrm{d}g(\omega), \\ \ddot{g}(t) = \int_{-\infty}^{\infty} C_g(\omega, t)\exp(\mathrm{i}\omega t)\,\mathrm{d}g(\omega) = \int_{-\infty}^{\infty}(\dot{B}_g(\omega, t) + \mathrm{i}\omega B_g(\omega, t))\exp(\mathrm{i}\omega t)\,\mathrm{d}g(\omega) \end{cases} \tag{20}$$

in which B_g and C_g denote the modulation functions of ground velocity and acceleration, respectively. The evolutionary cross-spectra of ground motions in Eq. (18) can therefore be expressed as

$$S_{lj}(\omega, t_1, t_2) = M_i^*(\omega, t_1)M_j(\omega, t_2)S_{g_l g_j}(\omega) \quad (g_l, g_j = u, v, w) \tag{21}$$

in which M_i is the modulation function of the lth component of ground motion, which could be A_g, B_g, or C_g depending on the type of the lth component, and $S_{g_l g_j}(\omega)$ is the cross-spectrum of the ground displacement at $t = 0$. Substituting Eq. (21) into Eq. (18) and letting $t_1 = t_2 = t$ yields the time-varying variance of the velocity

response v_k:

$$E(v_k^2(t)) = \int_{-\infty}^{\infty} \sum_l \sum_j \int_0^t h_{kl}(t-s_1) M_l^*(\omega, s_1) \exp(-\mathrm{i}\omega s_1)\,\mathrm{d}s_1),$$
$$\left(\int_0^t h_{kj}(t-s_2) M_j(\omega, s_2) \exp(\mathrm{i}\omega s_2)\,\mathrm{d}s_2 \right) S_{g_l g_j}(\omega)\,\mathrm{d}\omega. \tag{22}$$

The evolutionary spectrum of the velocity response $v_k(t)$ is given by

$$S_{v_k}(\omega, t) = \sum_l \sum_j H_{kl}^*(\omega, t) H_{kj}(\omega, t) S_{g_l g_j}(\omega) \tag{23a}$$

in which

$$H_{kl}^*(\omega, t) = \int_0^t h_{kl}(t-s_1) M_l^*(\omega, s_1) \exp(-\mathrm{i}\omega s_1)\,\mathrm{d}s_1, \tag{23b}$$

$$H_{kj}(\omega, t) = \int_0^t h_{kj}(t-s_2) M_j(\omega, s_2) \exp(\mathrm{i}\omega s_2)\,\mathrm{d}s_2. \tag{23c}$$

4.2. Modulation function

The modulation function of the evolutionary spectrum depends on both time and frequency. The explicit closed form of the modulation function of the evolutionary spectrum of traffic-induced ground motion is difficult to obtain. An approximate numerical approach is thus used in this study to compute the modulation function of the evolutionary spectrum. It is noted from Eq. (20) that the modulation functions of ground velocity and acceleration can be determined if the modulation function of the ground displacement is known. The first step in the numerical approach for determining the modulation function of the ground displacement is to divide the frequency range [0 ω_u] into n equal intervals $\Delta\omega$ by means of points $0 = \omega_0 < \omega_1 < \omega_2 < \cdots < \omega_{n-1} < \omega_n = \omega_u$, in which ω_u is the upper limit of the excitation spectrum $S_{g_j g_j}(\omega)_{(j=u,v,w)}$ and $\Delta\omega$ is equal to $\omega_f - \omega_{f-1}$ ($f = 1,2, \ldots, n$). Within each interval $[\omega_f - \omega_{f-1}]$, $S_{g_j g_j}(\omega)$ is assumed to vary linearly. The second step is to compute the ground displacement spectra $S_{g_j g_j}(\omega_f, t)$ based on Eq. (13) for a given time and given frequency. Finally, the modulation function of $S_{g_j g_j}(\omega)$ at the given time and frequency can be approximately expressed by

$$A_{g_j}(\omega_f, t) = \sqrt{\frac{S_{g_j g_j}(\omega_f, t)}{S_{g_j g_j}(\omega_f, 0)}}. \tag{24}$$

Repetition of the above steps for other frequencies and times yields the completed modulation function. Then, the modulation functions of the ground velocity and acceleration could be approximately calculated in terms of Eq. (20) with a simple difference method.

4.3. Application of BBN criteria

The BBN vibration criteria, in which the velocity response is adopted as a basis for estimating the microvibration level, are often used in assessing the environment influence upon the high-tech facilities. The one-third octave spectrum of any stationary velocity response time history $\dot{x}(t)$ can be expressed as

$$\dot{X}_{1/3}(n_c) = \left(\sum_{0.89 n_c}^{1.12 n_c} |\dot{X}(n)|^2 \Delta n \right)^{1/2}, \tag{25}$$

where $\dot{X}$is the FFT transform of the stationary velocity response, $\dot{X}_{1/3}$ the one-third octave spectrum, n the frequency in Hz, Δn the resolution of FFT, and n_c the centre frequency given by $n_c = 2^{m/3}$ (m is a positive integer). The application of BBN criteria often refers to stationary response, but the traffic-induced building

response in this study is non-stationary. In view of the fact that $E(|\dot{X}(n)|^2)$ equals the power spectrum $S_{\dot{x}}(n)$ of the velocity response $\dot{x}(t)$, $|\dot{X}(n)|^2$ in Eq. (25) could be replaced by the evolutionary spectrum $S_{\dot{x}}(n,t)$ so that Eq. (25) can be modified as

$$\dot{X}_{1/3}(n_c,t)=\left(\sum_{0.89n_c}^{1.12n_c} S_{\dot{x}}(n,t)\Delta n\right)^{1/2}. \tag{26}$$

5. Case study

This case study concerns a three-storey high-tech building located in proximity to a two-way one-lane roadway. The distance between the geometric centre of the building and the central line of the inner lane is about 35 and 42 m for the outer lane. The effects of traffic-induced ground motions on the normal operation of sensitive equipment housed in the building need to be assessed. In this connection, the spectra of both road roughness and vehicle force are first determined in accordance with the conditions of the concerned roadway and the traffic. The vehicle distribution along the roadway is generated in terms of the statistics of surveying data of vehicles running on the roadway. The frequency-response functions of the ground motions are determined based on the estimated soil properties, and the evolutionary spectra and modulation functions of the ground motions are then obtained and applied to the three-dimensional high-tech building. The effects of traffic-induced ground motions on the normal operation of sensitive equipment are finally assessed by comparing the computed velocity response spectra of the building floor with the modified BBN vibration criteria. Traffic-induced ground motions considered in the case study comprises both a single heavy truck and a traffic flow.

5.1. Road profile spectra and vehicle force spectra

The roadway concerned is a two-way one-lane asphalt roadway and the road condition can be approximately classified as level B as defined in ISO 8608 [16]. The relevant road parameters are 0.1 for the reference spatial frequency n_0 (cycles/m), 2 for the power exponent, and 64×10^{-6} for the amplitude of the displacement PSD function S_d (n_0) at n_0. Fig. 3 shows the spectrum of the road profile as a function of frequency in Hz by assuming that the velocity of the vehicles is 15 m/s. Vehicles running on the roadway can be classified as car, minibus, bus, truck, and heavy track. The dynamic parameters of each type of vehicles are listed in Table 1 and taken from Refs. [8,14], in which μ is the mass ratio m_2/m_1, F_b is the vehicle body-bounce frequency, F_h is the wheel-hop frequency, ξ_b and ξ_b are the viscous damping ratios of vehicle body and wheel,

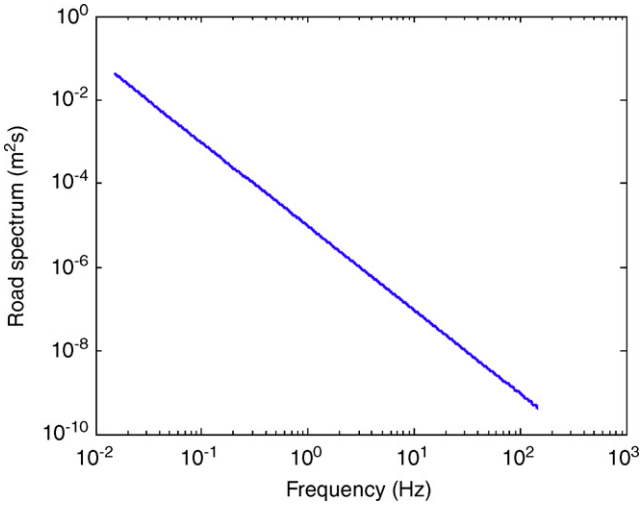

Fig. 3. Road profile spectrum.

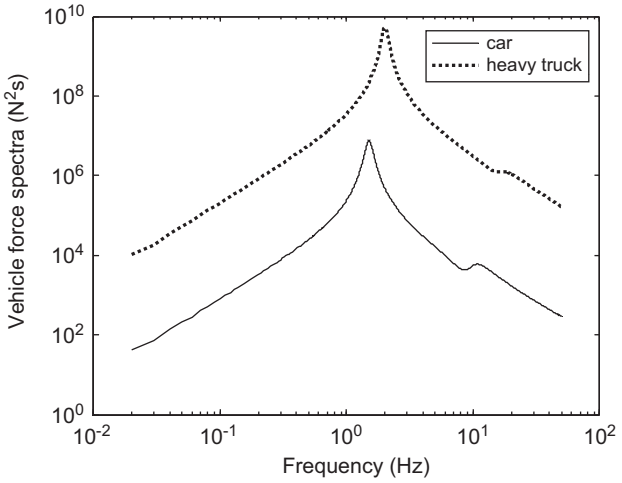

Fig. 4. Vehicle force spectra.

respectively. Fig. 4 presents the vertical force spectra of a car and a heavy truck subject to the road profile excitation characterized by the spectrum plotted in Fig. 3, which illuminates that the force spectral amplitude of the heavy truck is much greater than that of the car. There are two peaks in the vehicle force spectrum, in which the first peak corresponds to the vehicle body-bounce frequency and the second peak is related to the vehicle axle-hop frequency. Since the damping ratio of vehicle wheel is higher, the second spectral peak is smaller.

5.2. Vehicle distribution along the roadway

The 20-min traffic records of vehicles running on one lane of the roadway are analysed and shown in Table 2 for the number of vehicles from Monday to Saturday. The proportion of vehicle types is 42% for car, 23% for minibus, and 12% for bus, 15% for truck and 8% for heavy truck. The average traffic flow density λ is taken as 2.7 per 10 s while the average velocity of the traffic flow is assumed to be 15 m/s. The minimum reaction time for the drivers is 1 s, and the minimum threshold of spacing Δ_d is then determined as 15 m.

By using the method proposed in Section 2, the vehicle distributions on the two lanes of the roadway are generated and depicted in Fig. 5, in which the x-axis denotes the coordinates of vehicles in the queue while the y-axis is labelled with "c", "m", "b", "t", "h" to represent the vehicle type: car, minibus, bus, truck, and heavy truck, respectively. It is noted that the vehicles shown in Fig. 5(b) for the outer lane run in the opposite direction of the vehicles shown in Fig. 5(a) for the inner lane. The length of the traffic flows generated on the roadway is 1400 m, the mean spacing between the adjacent vehicles is 45 m and the total number of vehicles on one lane is about 21.

5.3. Frequency-response function

The parameters of the soil medium around the investigation area are summarized as follows: the soil density ρ is taken as 1800 kg/m^3; the shear module G is 7.2×10^7 N/m^2, the Poisson ratio v is 0.25; the soil damping ratio ξ is presumed to be 0.05. Correspondingly, the shear wave velocity C_s is 200 m/s; the compressive wave velocity C_p is 340 m/s; and the Rayleigh wave velocity C_R is 195 m/s. The frequency-response functions of the vertical and radial components of ground displacement caused by one single vertical harmonic point force are computed based on Eq. (11) for considering both body and Rayleigh wave effects. Figs. 6(a) and (b) depict the modulus of the frequency-response functions of the half-space in the vertical direction and the radial direction multiplied by a Gr as a function of the dimensional frequency $\bar{r}=\omega r/C_s$. It can be seen that within the lower

Table 2
Traffic records of Ye Licks on the roadway

Time (a.m.)	Mon	Tue	Wed	Thu	Fri	Sat
8:50–8:55	70	104	104	106	107	41
8:55–9:00	87	96	84	86	91	63
9:00–9:05	86	81	85	87	82	84
9:05–9:10	91	88	*25*	90	86	71

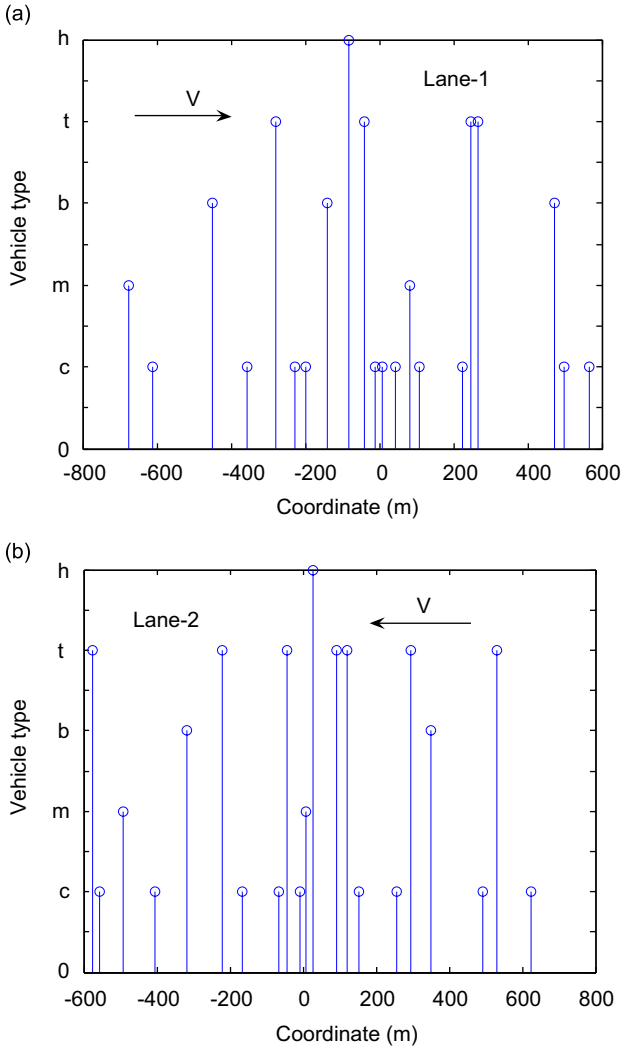

Fig. 5. Vehicle distribution along the roadway: (a) vehicle distribution along inner lane and (b) vehicle distribution along outer lane.

dimensionless frequency range or the shorter radial distance range, the consideration of Rayleigh wave effect only may underestimate the frequency-response function, in particular in the vertical direction. As the dimensionless frequency or the radial distance increases, the frequency-response function with only the Rayleigh wave effect included approaches that with both Rayleigh and body wave effects included.

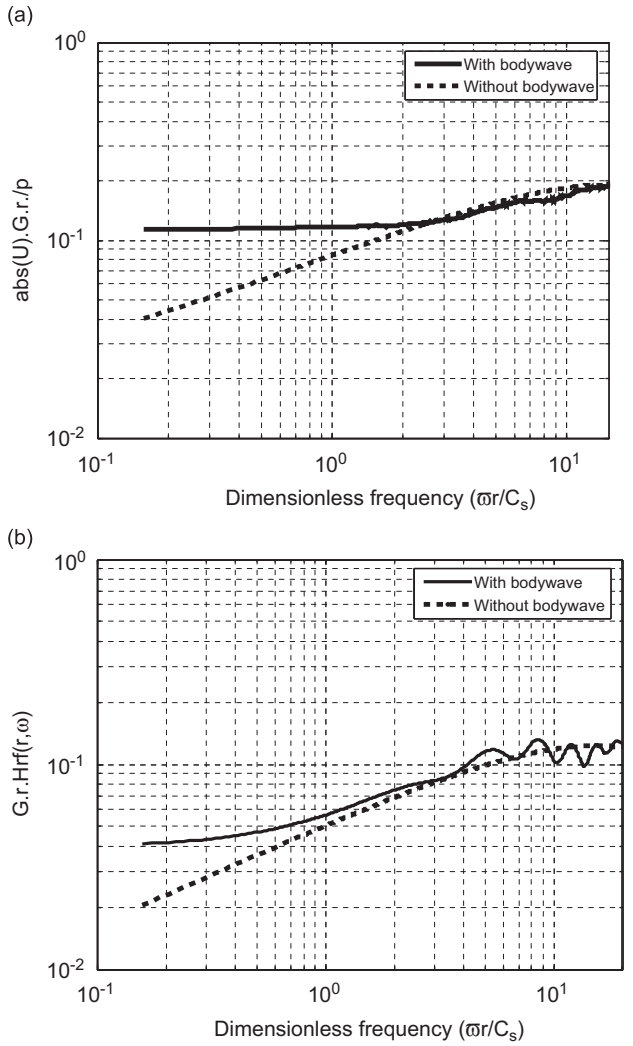

Fig. 6. Half-space frequency-response functions: (a) vertical displacement and (b) radial displacement.

5.4. Evolutionary ground displacement spectra

In consideration that the high-tech building is in proximity to the roadway, the ground responses at the investigation point caused by the vehicles running on the roadway are characterized by evolutionary ground spectra. The evolutionary ground displacement spectra and the associated modulation functions due to only one single heavy truck and one traffic flow are computed in this section in terms of Eqs. (13) and (24). The velocities of the single heavy truck and the traffic flow both are taken as 15 m/s. The vehicle distributions shown in Figs. 5(a) and (b) are used to represent the traffic flow. For the case of one single heavy truck, only the heavy truck on the inner lane as shown in Fig. 5(a) is considered. The vehicle parameters are listed in Table 1. The duration of the evolutionary spectra and the modulation function is taken as 10 s, and the time interval used in the computation is 0.02 s. The frequency range for the evolutionary spectra and the modulation function is from 1 to 40 Hz. The frequency interval used in the computation is 0.2 Hz. The evolutionary ground displacement response spectra in the z-direction (w-component) are shown in Fig. 7 for the time instant of 2, 3, 6, and 10 s, respectively. As can be seen from Fig. 7(a), the amplitudes of the ground displacement spectrum due to one single heavy truck at 6 s are larger than those at other times because the heavy vehicle is passing by the investigation point at that time. The peak of the evolutionary ground spectrum

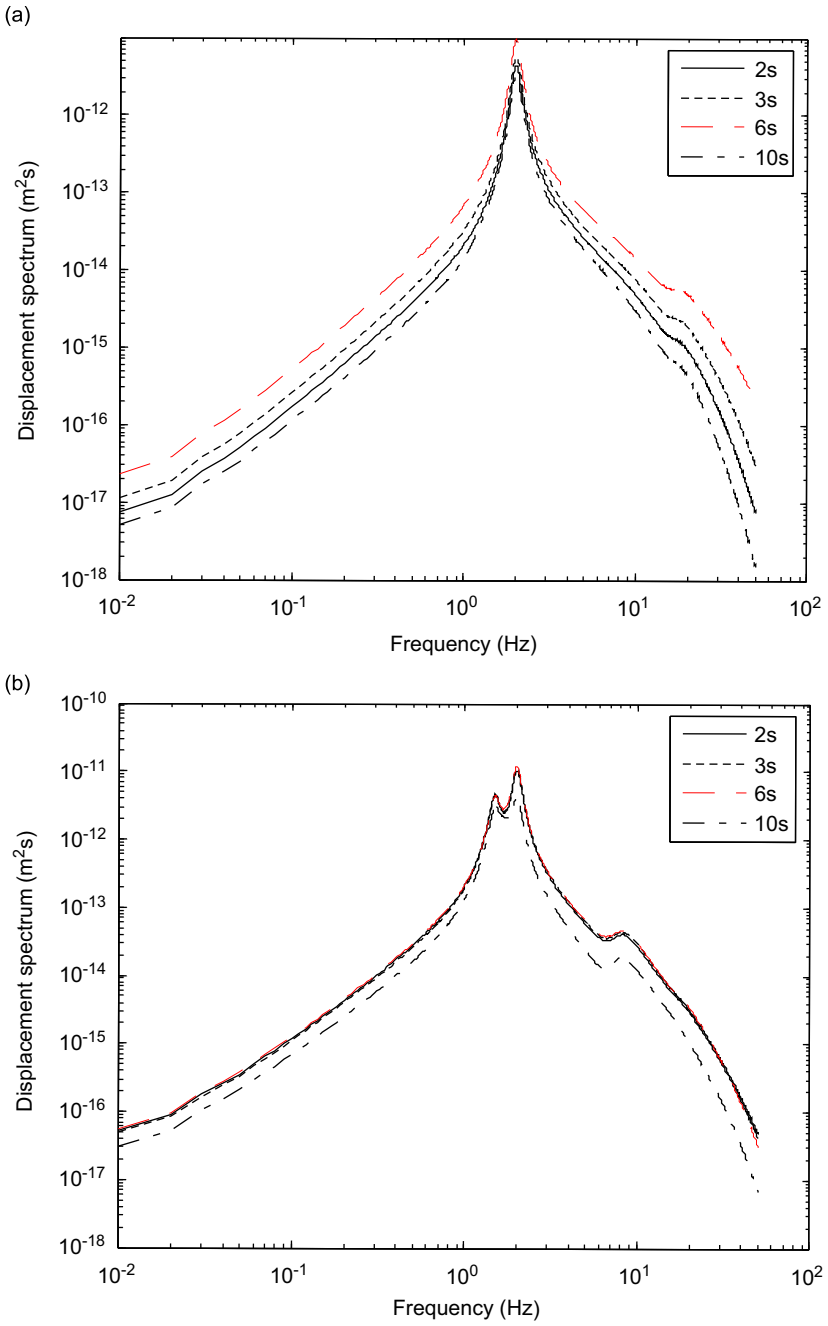

Fig. 7. Evolutionary displacement spectra (w-component): (a) single heavy truck and (b) traffic flow.

caused by one single heavy truck occurs at the frequency of 2 Hz, which coincides with the body-bounce frequency of the heavy truck. For the case of traffic flow, it can be seen from Fig. 7(b) that two peaks occur at the frequencies of about 1.5 and 2.0 Hz, which correspond to the body-bounce frequencies of the vehicles. The bandwidth of the ground response spectra caused by the traffic flow is wider than that due to the single heavy truck. The peak value of the ground response spectra caused by the traffic flow is also higher than that due to the single heavy truck. Fig. 8 plots modulation functions of the ground displacement spectra computed for the

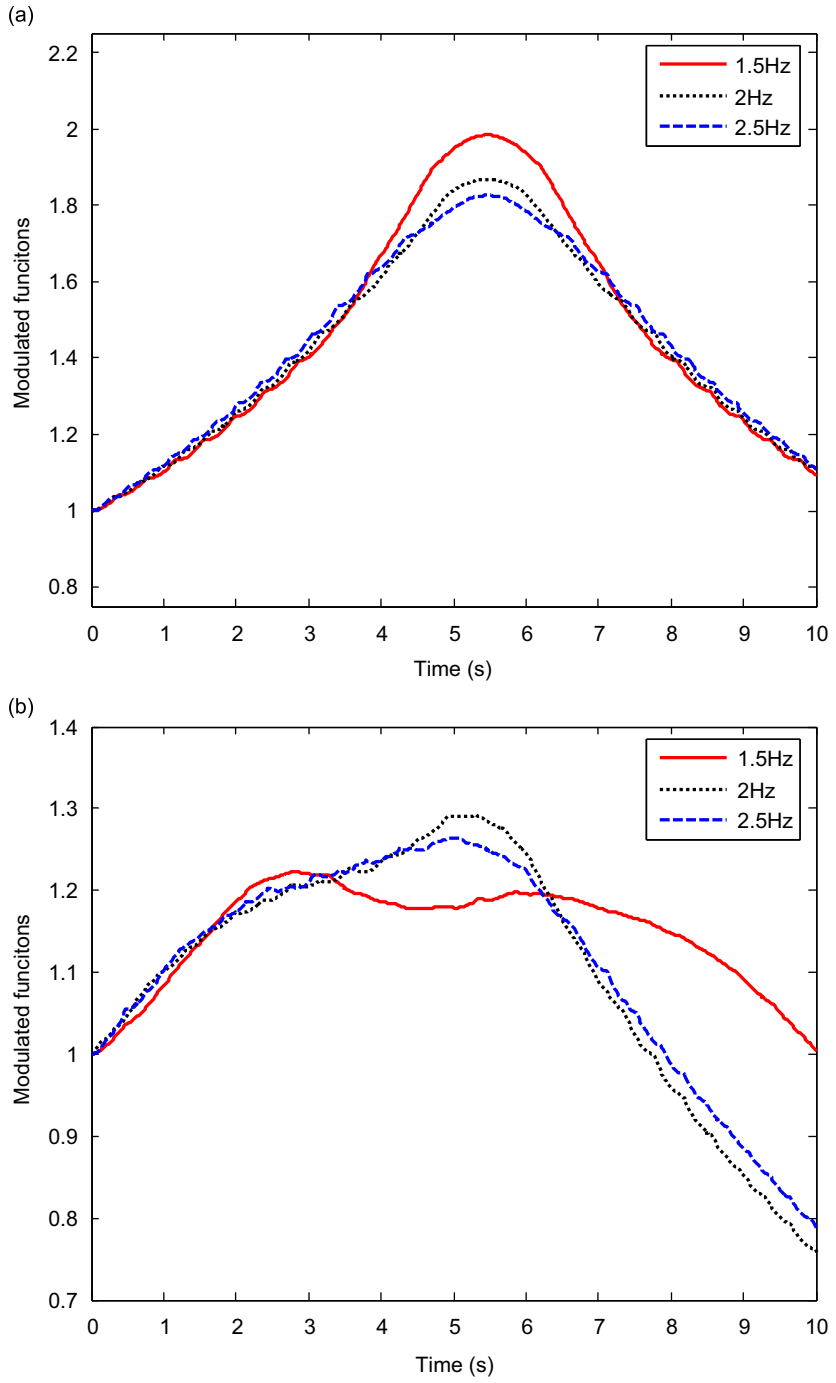

Fig. 8. Modulation functions of displacement spectra (w-component): (a) single heavy truck and (b) traffic flow.

investigation point in the z-direction (w-component) for the dominant frequencies of 1.5, 2.0, and 2.5 Hz. The modulation functions depicted in Fig. 8(a) are for the case of the single heavy truck while those in Fig. 8(b) are for the case of the traffic flow. It can be seen that the modulation functions for the case of single heavy truck are less affected by the frequency but the modulation functions for the case of the traffic flow are obviously frequency dependent within the concerned frequency range (1.5–2.5 Hz).

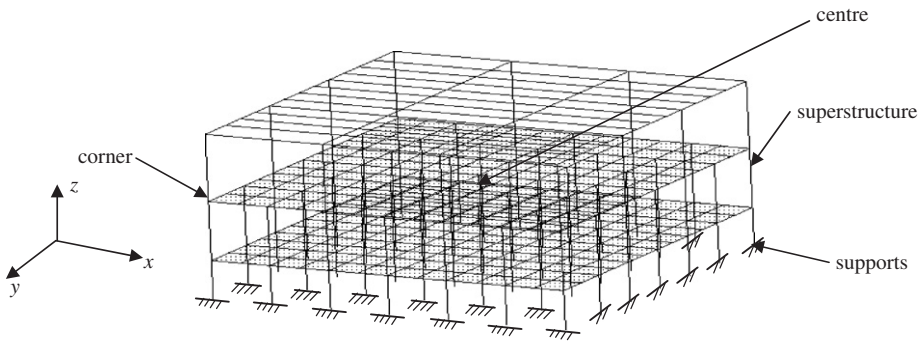

Fig. 9. Finite element model of the high-tech building.

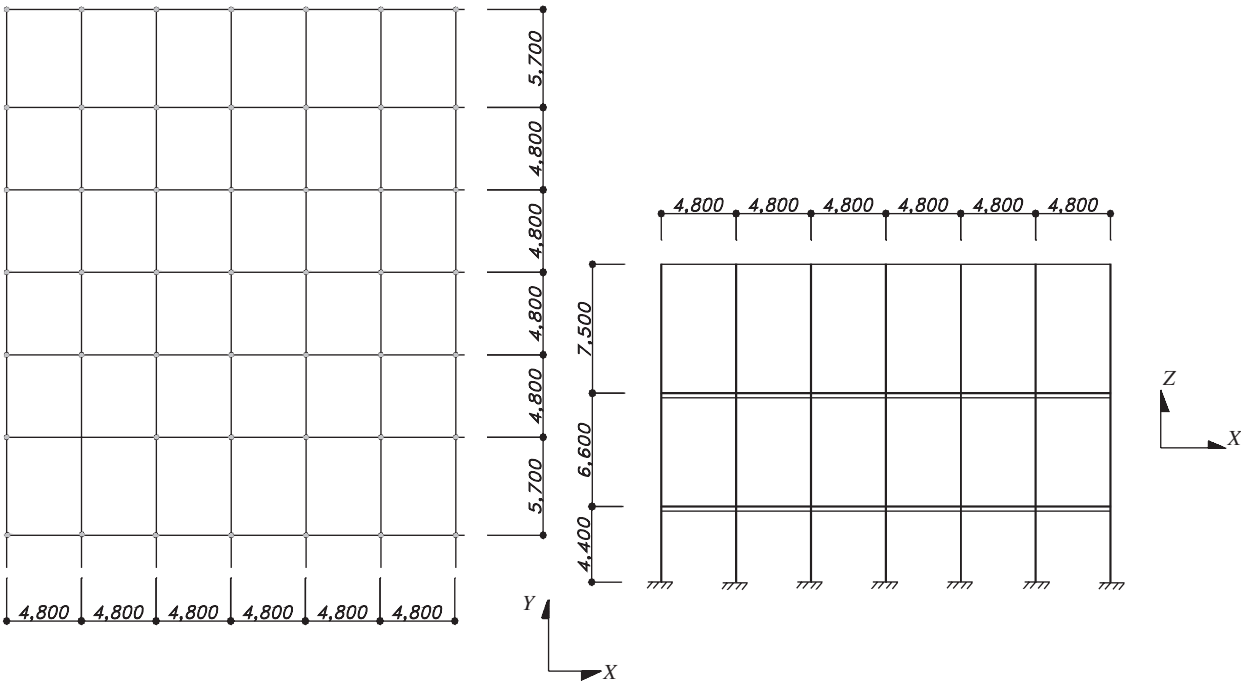

Fig. 10. Plane and elevation view of the high-tech building (unit: mm).

5.5. *High-tech building and finite element modelling*

For the three-storey high-tech building considered, its first and second stories are used as a double-level subfab and its third storey is used as a clean room. The clean room sits on the second floor supported by a series of columns that provide both the horizontal and vertical stiffness to the second floor. A vast quantity of high-tech equipment is installed on the second floor. A long truss spans over the clean room to form the building roof and to support mechanical equipment such as cranes for installation and maintenance. The horizontal stiffness of the columns supporting the truss is much smaller than that supporting the second floor. A finite element model with consistent mass matrix is established for the high-tech building, as shown in Fig. 9, in which all the beams and columns are modelled by six-degree-of-freedom (6 dof) beam elements while the floors are modelled by 24 dof shell elements, resulting in a total of 439 nodes and a total of 2634 dofs. The dimensions of the finite element model of the building in plane and elevation are given in Fig. 10. The density

and the modulus of elasticity of the concrete beams and columns are taken as $2700\,kg/m^3$ and $3\times10^{10}\,Pa$, respectively. The average thickness of the first floor and the second floor are all 0.25 m. The modal analysis shows that the first natural frequency of 1.98 Hz corresponds to the first lateral mode shape in the x-direction whereas in the y-direction, the first natural frequency is 4 Hz.

5.6. Traffic-induced building response

To gain a full insight into traffic-induced building vibration, the absolute velocity responses of the high-tech facility due to the single heavy truck and the traffic flow are both studied in this section. Since the clean room is located on the second floor of the building, the absolute velocity responses at the centre of the second floor in the x-, y-, and z-direction are computed and discussed. The evolutionary velocity spectra are obtained in terms of Eq. (23), in which the frequency ranges, the time durations together with their resolutions employed are the same as used in the generation of the evolutionary ground motion spectra.

Figs. 11(a) and (b) present the evolutionary spectra of the absolute velocity at the centre of the second floor of the building in the z-direction (the w-component) at the time instant of 2, 3, 6, and 10 s due to the single heavy truck and the traffic flow, respectively. For the case of the single heavy truck, the significant variation of the building velocity spectrum with time can be observed clearly from Fig. 11(a). At the 2nd second, the peak value of the velocity spectrum is about $0.75\times10^{-9}\,m^2/s$, but the peak value reaches approximately its maximum value of $1.6\times10^{-9}\,m^2/s$ at the 6th second because the heavy truck passes by the building at that instant. As the heavy vehicle runs away from the building, the peak value of the velocity spectrum reduces to $0.5\times10^{-9}\,m^2/s$ at the 10th second. The significant variation of the building velocity spectrum indicates a remarkably non-stationary property. Also observed from Fig. 11(a) are two dominant frequencies around 2 and 13 Hz, which correspond to the dominating frequency of the ground motion and the natural frequency of the building in the vertical direction. The resonance of the second floor in the vertical direction is therefore small.

For the case of the traffic flow, the two predominant frequencies in the evolutionary spectra remain the same as those in the case of the single heavy truck, but the two maximum peak values of the spectrum are much larger than those due to the single heavy truck. This is because the building response is caused by all the vehicles passing nearby. The variation of velocity spectrum with time for the case of the traffic flow is not as significant as that for the case of the single heavy truck. For instance, the peak value of the velocity spectrum shown in Fig. 11(b) is about $1.8\times10^{-9}\,m^2/s$ at the 2nd second whereas the peak value at the 6th second is about $2.2\times10^{-9}\,m^2/s$.

Figs. 12 and 13 display the evolutionary spectra of the absolute velocity at the centre of the second floor of the building in the x- and y-direction (the u- and v-component), respectively, at the time instant of 2, 3, 6, and 10 s due to the single heavy truck and the traffic flow. The similar observations to the w-component can be made for the u- and v-component, that is, the variation of the velocity spectrum with time is more significant for the case of the single heavy vehicle than for the case of the traffic flow. Furthermore, there are more peaks in the velocity spectra for the x-direction and the y-direction than for the z-direction. Like in the z-direction, the first dominant frequency in the velocity spectra for the x- and y-direction corresponds to the dominant frequency in the ground motion spectra for the x- and y-direction, respectively. Apart from the first dominant frequency, the other dominant frequencies in the velocity spectra for the x-direction and the y-direction are different from those for the z-direction. These phenomena are mainly because the natural frequencies of the building in the x-direction and the y-direction are different from those in the z-direction. It is also noted that the evolutionary spectrum reaches its maximum in the x-direction at the 3rd second but in the y- and z-direction at the 6th second. This is because the ground motion in the x-direction at the building location is actually parallel to the motion direction of the vehicles. When the vehicles pass by the building, the ground motion in the x-direction at the building location becomes small so that the maximum value in the velocity spectrum for the x-direction does not occur at the moment when the vehicles pass by the building. It is also observed that the maximum value of the spectrum in the x-direction is much smaller than that in the z-direction. For instance, the maximum value of the spectrum in the x-direction for the case of the traffic flow is less than $7\times10^{-10}\,m^2/s$ whereas the counterpart in the z-direction is about $22\times10^{-10}\,m^2/s$, which further supports the preceding explanation.

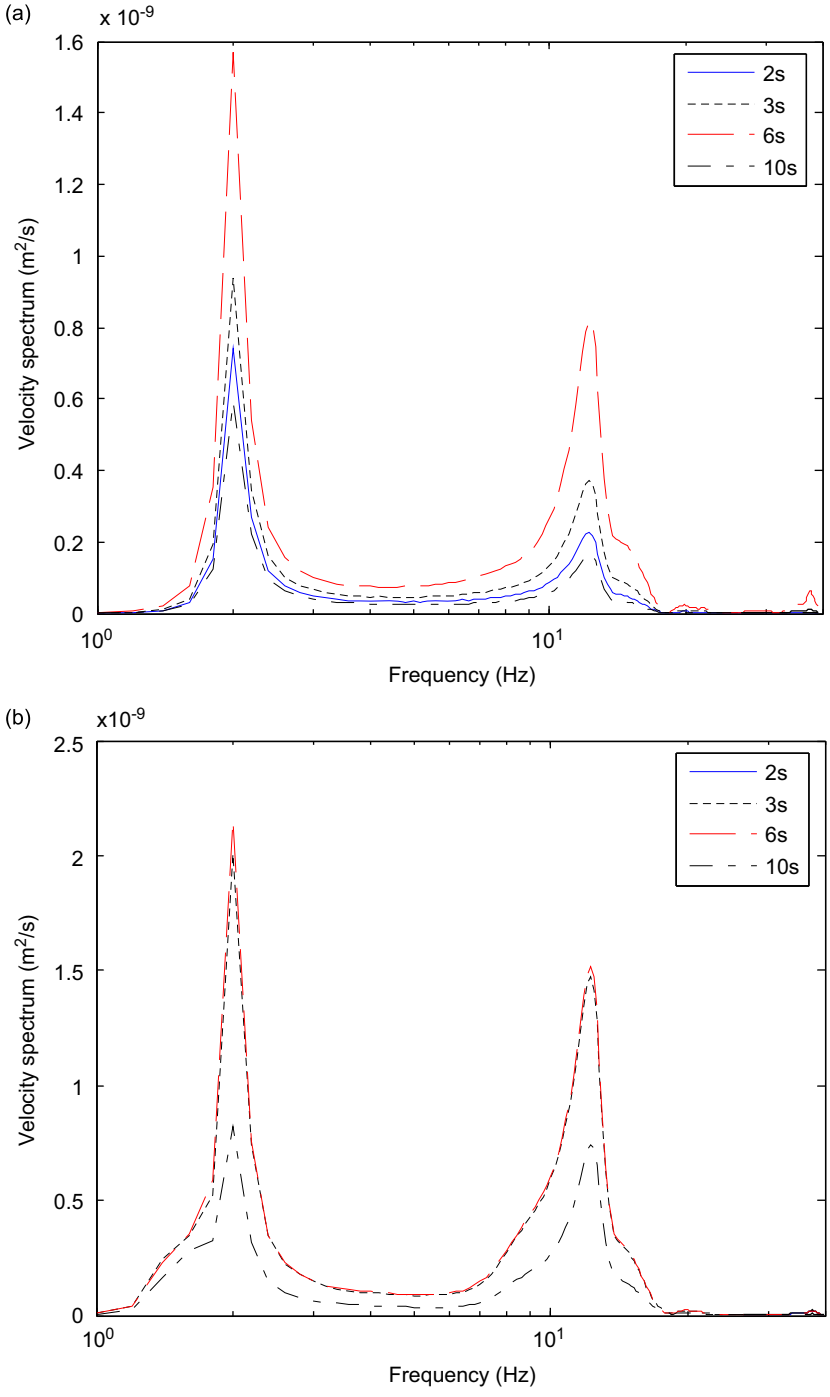

Fig. 11. Velocity response spectra of the second floor at centre (*w*-component): (a) single heavy truck and (b) traffic flow.

In accordance with the BBN criteria, the maximum spectrum in each direction is converted to the one-third octave band velocity spectrum and compared with the BBN criteria. The one-third octave band velocity response spectra at the centre of the second floor of the building in the three directions are depicted in Fig. 14(a) for the case of the single heavy truck and in Fig. 14(b) for the case of the traffic flow. It can be observed that the vibration levels of the second floor all exceed the VC-E level specified for the

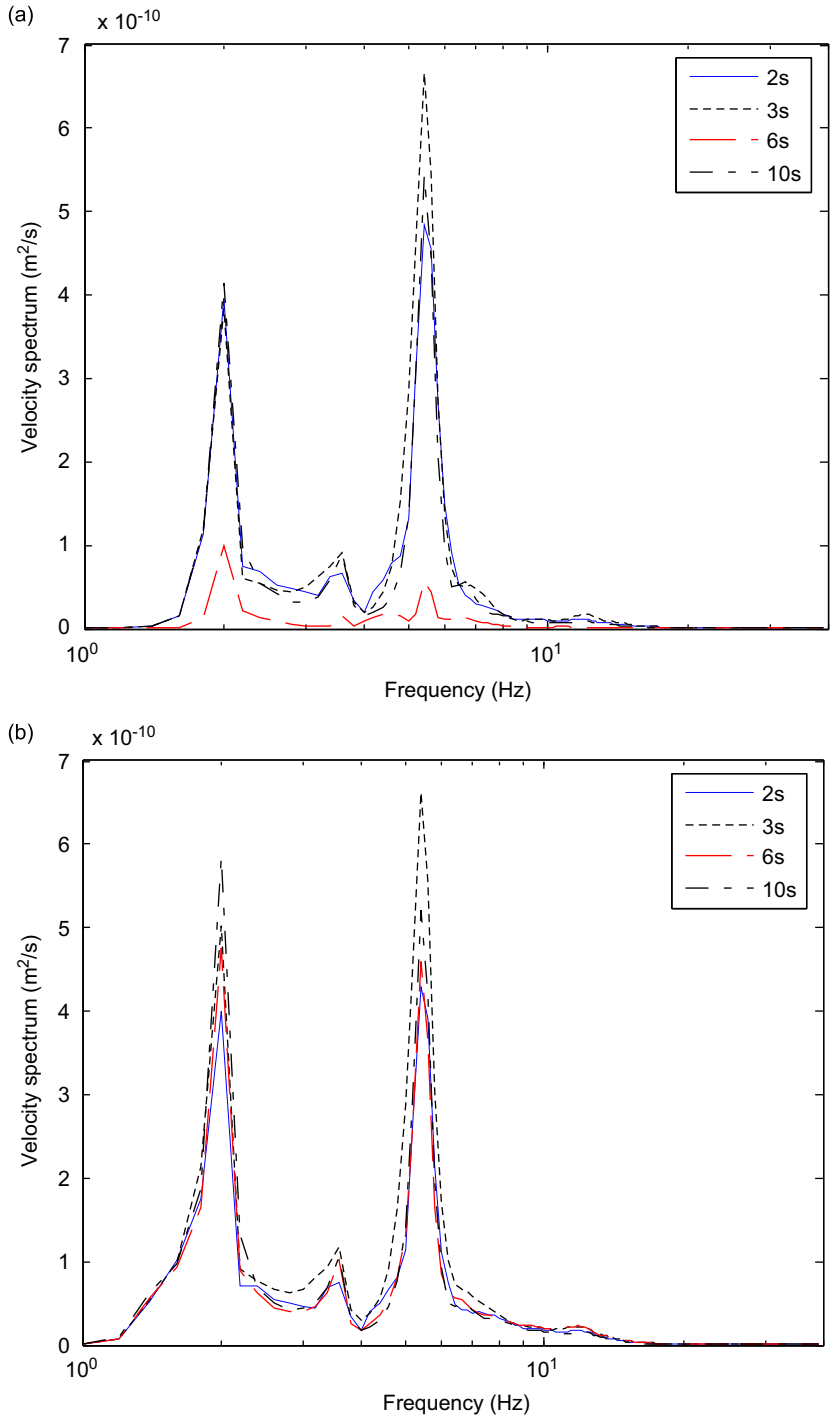

Fig. 12. Velocity response spectra of the second floor at centre (u-component): (a) single heavy truck and (b) traffic flow.

extremely sensitive equipment. The vibration levels caused by the traffic flow are higher than those by the single heavy truck. For a given traffic condition, the vibration level in the z-direction is the highest among the three directions. Hence, some measures shall be employed to mitigate traffic-induced building vibration.

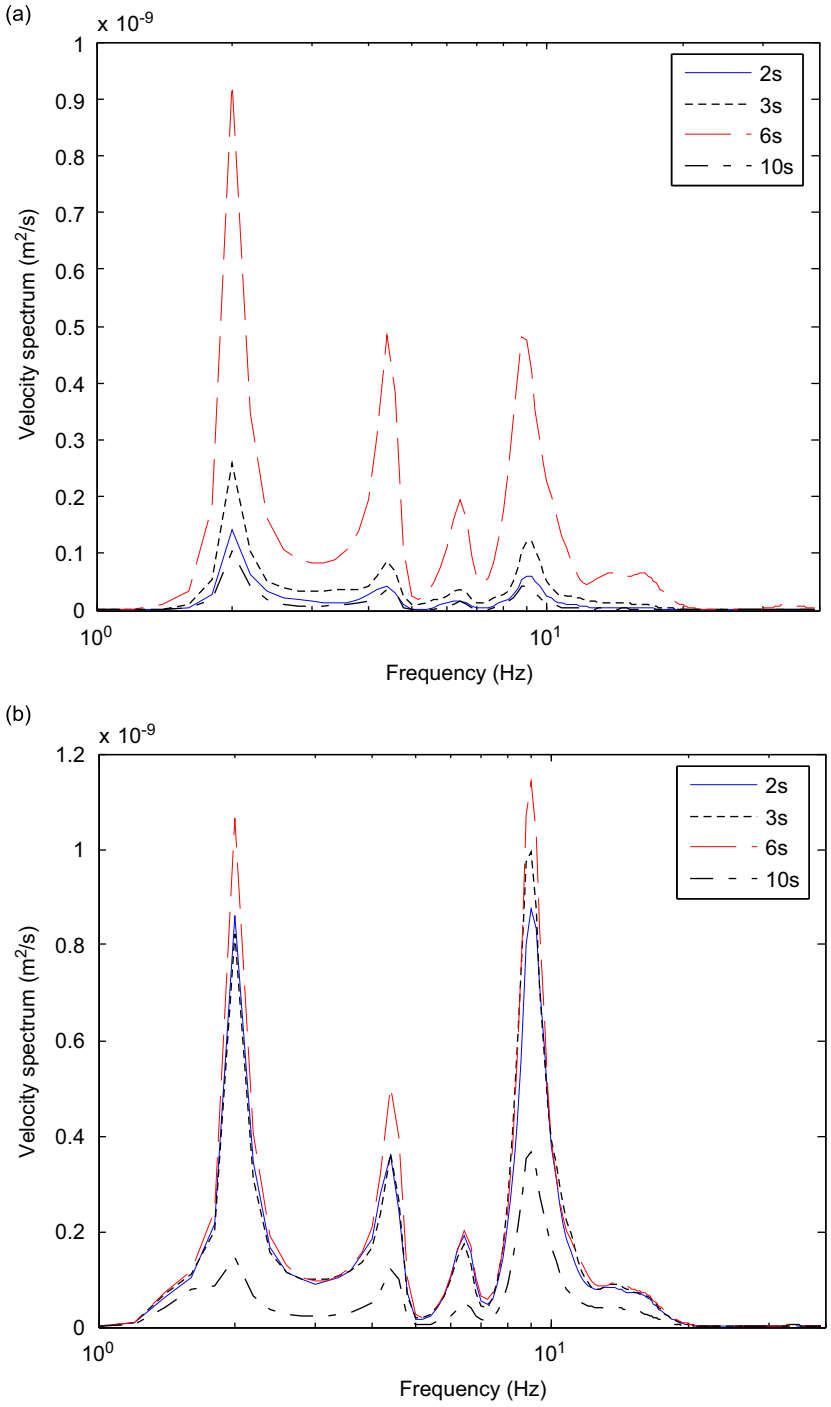

Fig. 13. Velocity response spectra of the second floor at centre (v-component): (a) single heavy truck and (b) traffic flow.

It should be pointed out that this investigation is a preliminary study, which does not consider the effects of soil–structure interaction (SSI) and wave passage on the building response caused by traffic-induced ground motion. Although the effects of SSI and wave passage on the building response caused by earthquake induced ground motion have been studied extensively, the study on the counterpart caused by traffic-induced ground

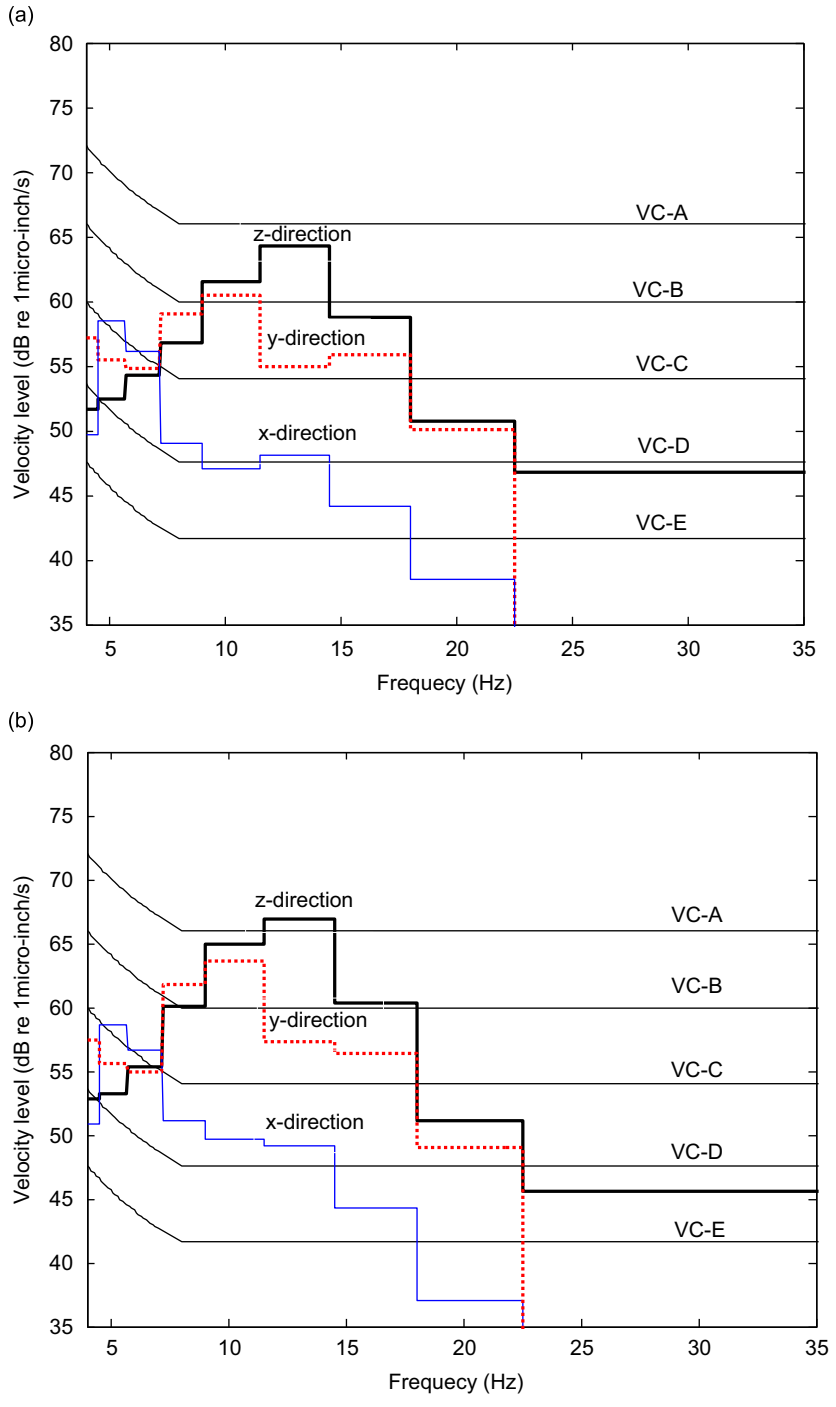

Fig. 14. One-third octave band velocity spectra of the second floor at center: (a) single heavy truck and (b) traffic flow.

motion is very limited. This is partially because the ground motion induced by traffic is often much smaller than that induced by earthquake and the SSI in the case of traffic is not as significant as that in the case of earthquake. This is particularly true when the high-tech building foundation sits on stiff soil. Nevertheless, the effects of SSI and wave passage on the building response caused by traffic-induced ground motion deserve further study.

6. Concluding remarks

The framework for quantifying building responses to traffic-induced ground motions has been presented in this study. The framework involves the simulation of vehicle distribution along a roadway, the consideration of both Rayleigh and body wave effects on traffic-induced ground motion, the development of evolutionary ground response spectra, and the quantification of evolutionary response spectra of three-dimensional buildings in close proximity to the roadway. A case study using a typical high-tech building in proximity to a roadway has been conducted using the proposed framework. The effects of two traffic conditions, a single heavy truck and a traffic flow, have been investigated. The results show that within lower dimensionless frequency range or shorter radial distance range, the consideration of Rayleigh wave effects only may underestimate the ground frequency-response function and the ground displacement spectra. The results also show that the velocity responses of the high-tech building due to the traffic flow are larger than those due to the single heavy truck. The case study finally uncovered that the traffic-induced ground motions impede the normal operation of sensitive equipment housed in the building, and some measures should be taken to reduce traffic-induced vibration. It is worthwhile to pint out that the SSI and the spatial variation of ground motions among the building supports are ignored in this study and shall be investigated in the near future.

Acknowledgement

The writers are grateful for the financial support from the Research Grants Council of Hong Kong through a CERG Grant (PolyU 5054/02E).

References

[1] L. Auersch, Wave propagation in layered soil dynamics: theoretical solution in wave number domain and experimental results of hammer and railway traffic excitation, *Journal of Sound and Vibration* 173 (1994) 233–264.
[2] T. Hanazato, K. Ugai, Analysis of traffic induced vibrations by FEM, *Journal of Japanese Society of Soil Mechanics and Foundation Engineering* 23 (1983) 144–150.
[3] G. Lombaert, G. Degrande, D. Clouteau, Numerical modelling of free field traffic-induced vibrations, *Soil Dynamics and Earthquake Engineering* 19 (2000) 473–488.
[4] D. Clouteau, G. Degrande, G. Lombaert, Numerical modelling of traffic induced vibrations, *Meccanica* 36 (2001) 401–420.
[5] S. Francois, G. Lombaert, G. Degrande, Local and global shape functions in a boundary element formulation for the calculation of traffic induced vibrations, *Soil Dynamics and Earthquake Engineering* 25 (2005) 839–856.
[6] H.E.M. Hunt, Modelling of road vehicles for calculation of traffic-induced ground vibration as a random process, *Journal of Sound and Vibration* 144 (1991) 41–51.
[7] H.E.M. Hunt, Stochastic modeling of traffic-induced ground vibration, *Journal of Sound and Vibration* 144 (1991) 53–70.
[8] H. Hao, T.C. Ang, Analytical modelling of traffic-induced ground vibrations, *Journal of Engineering Mechanics—ASCE* 124 (1998) 921–928.
[9] H. Hao, T.C. Ang, J. Shen, Building vibration to traffic-induced ground motion, *Building and Environment* 36 (2001) 321–336.
[10] G.R. Watts, V.V. Krylov, Ground-borne vibrations generated by vehicles crossing road humps and speed control cushions, *Applied Acoustics* 59 (2000) 221–236.
[11] Y.L. Xu, A.X. Guo, Microvibration control of coupled high tech equipment-building systems in vertical direction, *International Journal of Solids and Structures* 43 (2006) 6521–6534.
[12] H. Amick, On the generic vibration criteria for advanced technology facilities, *Journal of the Institute of Environmental Sciences* XL (1997) 35–44.
[13] D. Heidemann, H. Wegmann, Queueing at unsignalized intersections, *Transportation Research B* 31 (1997) 239–263.
[14] C.E. Reynolds, J.C. Steedman, *Reinforced Concrete Designer's Handbook*, A Viewpoint Publication, London, 1981.
[15] W.L. Martinez, A.R. Martinez, *Computational Statistics Handbook with Matlab*, Chapman & Hall CRC, Washington, DC, 2002.
[16] ISO 8608, *Mechanical Vibration—Road Surface Profiles—Reporting of Measured Data*, 1995.
[17] H. Lamb, On the propagation of tremors over the surface of an elastic solid, *Philosophical Transactions of the Royal Society Series A London* 203 (1907) 1–42.
[18] U. Holzlohner, Vibrations of the elastic half-space due to the vertical surface loads, *Earthquake Engineering and Structural dynamics* 8 (1980) 405–414.
[19] A.K. Chopra, *Dynamics of Structures: Theory and Applications to Earthquake Engineering*, second ed., Pearson Education Inc. & Prentice-Hall, Englewood Cliffs, NJ, 2001.
[20] M.B. Priestley, Power spectral analysis of non-stationary random processes, *Journal of Sound and Vibration* 6 (1967) 86–97.